Environmental and Experimental Botany 243 (2026) 106334

Contents lists available at ScienceDirect

Environmental and Experimental Botany

journal homepage: www.elsevier.com/locate/envexpbot

Research paper

Key regulators of floral induction in faba bean (*Vicia faba* L.) are revealed from spatio-temporal gene expression analysis of contrasting genotypes

Umer Mahmood *, Per Hofvander, Åsa Grimberg

Department of Plant Breeding, Swedish University of Agricultural Sciences (SLU), Lomma SE-234 22, Sweden

ARTICLE INFO

Dataset link: Transcriptome profiling of shoot apex and leaf tissues reveals regulatory networks controlling flowering time in Vicia faba

Keywords:
Vicia faba
Floral induction
Protein crop
Legume
Co-expression
Gibberellin
Photoperiod

ABSTRACT

Flowering time is a crucial trait for crop adaptation and yield stability, yet its genetic regulation in *Vicia faba* remains poorly understood. In this study, we performed RNA-sequencing of shoot apex (SA) and leaf tissues to investigate the genetic mechanisms underlying variation in flowering time between two contrasting cultivars, Gubbestad (early flowering) and Honey (late flowering). Based on differential gene expression analysis, *K*-means clustering and weighted gene co-expression network analysis (WGCNA), we identified key transcriptional modules enriched in genes associated with gibberellin (GA) signaling, photoperiod response, and floral induction. Notably, *FT* homologs exhibited distinct expression patterns: two *FT* genes were expressed in Gubbestad, whereas only one was detected in Honey, in the SA during the reproductive stage. The late-flowering cultivar displayed high expression of the transcriptional cofactor *TFL1* and transcription factor *AP2* in the SA at the vegetative stage, which likely contributed to late floral initiation by suppressing downstream activators of flowering such as *SOC1*, *AP1*, and *SPL*/miR156. In contrast, the early-flowering cultivar showed *FT* gene expression in both leaf and SA, promoting *LFY*, *SOC1* which accelerate floral transition. Through co-expression analysis, WGCNA identified *SOC1* and *AG* as key hub genes within flowering-related modules, co-expressed with multiple genes encoding regulators of floral development. Our findings highlight the interplay between GA-mediated flowering pathways and photoperiod-responsive genes, revealing a complex regulatory network that controls floral induction. Unraveling these molecular mechanisms provides insights into breeding faba bean cultivars that are better adapted to different geographical regions.

1. Introduction

Faba bean (*Vicia faba L.*, 2 n = 12) is an important legume crop used for human consumption and livestock feed (Yu et al., 2023). Faba bean is one of the oldest domesticated crops, with evidence of its cultivation dating back 10,0000 BP in northwestern Syria (Karkanis et al., 2018). Global production has increased by about 30 % over the past decade (2012–2022) (FAOSTAT, 2024). Yet European grain legume production remains relatively low despite a growing demand for locally produced plant-based protein sources for food and feed (Jensen et al., 2021). Environmental factors, such as short growing season and cooler climates, limit the warm season legumes (e.g., soybeans) in Northern Europe. However, faba bean has shown good adaptability (De Notaris et al., 2023), therefore, the development of early-flowering cultivars is crucial for expanding cultivation to northern latitudes. This is pivotal since the need for locally produced plant-based protein is increasing in Scandinavia (Bunge et al., 2024).

Faba bean is a cool season legume that plays a vital role in sustainable cropping systems by crop rotation and reducing the use of synthetic fertilizers through its nitrogen fixation ability (De Notaris et al., 2023; Mesfin et al., 2020; Ohm et al., 2024). Apart from its agronomic importance, faba bean is highly nutritious, containing 25–40 % protein, 47–68 % carbohydrates, and 11–30 % fiber (Augustin and Cole, 2022; Hall et al., 2017). Furthermore, the rising demand for plant-based proteins and sustainable agricultural practices are in accordance with the UN Sustainable Development Goals that encourage a shift to plant-based diets (Augustin and Cole, 2022). Despite this, faba bean remains an underutilized crop globally, with 2 % of the global soybean output in 2022 (FAOSTAT, 2024). According to recent reports faba bean cultivation in Sweden covers only less than 1 % of arable land

* Corresponding author.
E-mail address: umer.mahmood@slu.se (U. Mahmood).

https://doi.org/10.1016/j.envexpbot.2026.106334
Received 4 August 2025; Received in revised form 29 January 2026; Accepted 21 February 2026
Available online 23 February 2026

(Jordbruksverket, 2024). The short growing seasons and cooler climates at Nordic latitudes are limiting factors for cultivation, emphasizing the need for varieties adapted to regional conditions.

Flowering time is an important trait in crop adaptation to local environments and yield improvement (Wu et al., 2023). This is orchestrated by a complex interplay between external environmental signals and internal genetic regulators (Hu et al., 2020). Six major regulatory pathways govern the transition to flowering in Arabidopsis: vernalization, photoperiod, autonomous, gibberellin, sugar metabolism, and age dependent pathways (Blümel et al., 2015; Wellmer and Riechmann, 2010). These pathways coordinate the regulation of key flowering genes, including *CONSTANS* (*CO*), *FLOWERING LOCUS T* (*FT*), *SUPPRESSOR OF OVEREXPRESSION OF CO 1* (*SOC1*), *FLOWERING LOCUS C (FLC)*, *LEAFY* (*LFY*), and *APETALA (AP1*, *AP2*, *AP3*), facilitating the transition from vegetative to floral meristem formation (Rehman et al., 2023). *LFY* is one of the primary genes induced in floral primordia and works alongside the E3 ubiquitin ligase *UNUSUAL FLORAL ORGANS* (*UFO*) (Dolde et al., 2023; Hempel et al., 1997). Together with *AP1* and *CAULIFLOWER* (*CAL*), it determines floral meristem identity, whereas *AGAMOUS-like* (*AGL24*), *SOC1*, and *SHORT VEGETATIVE PHASE* (*SVP*) contribute to the maintenance of this state during the early stages of development (Quiroz et al., 2021). The MADS-box *FLC* acts as a flowering repressor by delaying the expression of *SOC1* and *FT* in leaves and inflorescence meristems. Vernalization reduces its activity, thereby facilitating flowering through a gradual decrease in FLC transcript and protein levels (Shi et al., 2024; Moon et al., 2003). In Arabidopsis, long-day flowering is regulated by the CO-FT photoperiod module, as CO directly activates *FT* by binding to its promoter (Lv et al., 2021). Subsequently, FT moves to the shoot apex and forms the FT-FD complex to promote floral meristem identity. This complex also represses *FLC* in a feedback loop that is crucial for coordinating flowering time and maintaining seed dormancy (Luo et al., 2019). Additionally, SVP interacts with FLC or functions independently to regulate flowering genes, including *TEMPRANILLO 1* (*TEM1*), *CO-like* (*COL1/4*), *SEPALLATA 3* (*SEP3*), and ethylene-responsive *SCHLAFMUTZE* (*SMZ*) (Quiroz et al., 2021). SVP can also bind separately to *FT* and *SOC1* (Mateos et al., 2015). Other MADS-box repressors, such as AGL15 and AGL18 suppress flowering through *FT* and *SOC1*, while microRNAs miR156 and miR172 are crucial in age-dependent flowering regulation (Adamczyk et al., 2007; Fernandez et al., 2014; Serivichyaswat et al., 2015). The gradual decline of miR156 allows SQUAMOSA PROMOTER BINDING PROTEIN-LIKE (SPL) to accumulate, promoting flowering through the activation of miR172B, which represses *AP2-like* genes and enables *SPL3/4/5* activity (Hyun et al., 2017; Mateos et al., 2015; Quiroz et al., 2021). In addition, *SPL3* directly regulates FT expression in leaves to promote flowering in response to ambient temperature (Kim et al., 2012). Conversely, *SMZ* represses SOC1 and *AP1* to maintain floral inhibition through a feedback manner (Tao et al., 2012).

In legumes, *FT* homologs *(FTa*, *FTb*, and *FTc*) were previously reported to have distinct expression patterns. In pea, expressions of *FTa1 and FTb2* act as key signals for floral induction, with *FTb2* being induced in leaves under long days, whereas *FTa1* and *FTc* are expressed in the apical meristem. *FTa1* triggers flowering without photoperiod sensitivity, whereas *FTb2* initiates the primary signal in leaves (Aguilar-Benitez et al., 2021; Yoo et al., 2010). Despite progress made in pea and soybean (Weller and Ortega, 2015), flowering regulators in other legumes, including faba bean, remain largely unexplored.

Faba bean is generally classified as a day-neutral plant, although some accessions require long-day conditions for flowering (Patrick and Stoddard, 2010). However, flowering is primarily driven by thermal time and winter types require vernalization to initiate reproductive development (Karkanis et al., 2018). A recent study showed that vernalization responsive legumes, including winter types of *V. faba*, generally lack a homolog of the Arabidopsis floral repressor FLC (Surkova and Samsonova, 2022), indicating that cold mediated repression in legumes operates through an alternative mechanism. In a transcriptomic study of *V. faba*, *CO* signaling related genes (e.g; *COL5*, *CRYPTOCHROME1*), have been identified under cold treatment (Yuan et al., 2021). In the absence of *FLC,* repression of floral induction in legumes is mediated by *VERNALIZATION2* (*VRN2*) regulators, such as *MtVRN2* in Medicago, which directly represses *FTa1* (Jaudal et al., 2016). A key floral activator *SOC1*, identified in *V. faba*, showed vernalization mediated expression and promoted earlier flowering when ectopically expressed in Arabidopsis (Yuan et al., 2021). Despite these findings only a few studies have investigated flowering time regulation in faba bean (Catt et al., 2017; Yuan et al., 2021; Ohm et al., 2025), underscoring the need for further characterization of its flowering pathways.

Understanding the genetic regulation of flowering time is important for breeding high-yielding, climate-resilient cultivars suitable for different geographical regions and environments. In the current transcriptomic study, we analyzed two cultivars with contrasting flowering times. Using *K*-means clustering and WGCNA, we identified key regulatory pathways and candidate genes involved in floral induction, providing novel insights into the genetic control of flowering time in faba bean.

2. Material and methods

2.1. Plant material and phenotype measurements

Two indeterminate *Vicia faba* cultivars with contrasting flowering times, Gubbestad (early) and Honey (late), were selected based on the results of a previous field trial (Ohm et al., 2024) and a preliminary growth chamber experiment (Biotron, SLU-Alnarp). Both cultivars were grown in 7.5 L pots containing commercial planting soil (Blom och Plantjord, Cramers Blommor) supplemented with 2 g/L of controlled release fertilizer (Osmocote 5, 5–6 M, ICL). Plants were maintained under fluorescent light (200 $\mu mol \cdot m^{-2} \cdot s^{-1}$) in controlled climate chambers (Biotron, SLU-Alnarp) under a 16/8 h light/dark cycle with 20°C/18°C day/night temperature and 60 % humidity. Flowering initiation was recorded when the first flower opened in each cultivar.

2.2. RNA sequencing and identification of DEGs

Shoot apex (SA) and leaf tissues (uppermost mature leaf; relevant for photoperiod related signaling) from both cultivars were harvested at three time points for RNA sequencing. These were carefully selected to represent distinct biological phases of the floral transition. The first time point (21 days after sowing, DAS) corresponded to the vegetative stage before any morphological signs of reproductive development. The second time point (39 DAS) coincided with visible sign of floral initiation in the early-flowering cultivar (Gubbestad), capturing the onset of reproductive transition. The third time point (68 DAS) represented the corresponding phase of floral initiation in late-flowering cultivar (Honey), enabling direct comparison with the early flowering cultivar Gubbestad. All samples were collected at the same time of the day (6–7 h after the start of the light period) to ensure that samples represented the same time point during the diurnal rhythm. In total, 36 samples (2 tissues × 2 cultivars × 3 stages × 3 biological replicates) were collected for transcriptomic analysis. Total RNA was extracted using the PureLink™ Plant RNA Reagent, and residual genomic DNA was removed using the TURBO DNA-free™ Kit (Cat. No. AM1907). Kits were supplied by Invitrogen (Thermo Fisher Scientific; USA) and followed the manufacturer protocol. NanoDrop spectrophotometer and Agilent 2100 Bioanalyzer were then used for RNA quality assessment. cDNA libraries were prepared using polyA-enriched mRNA and sequenced using the INVIEW Transcriptome Discover service on the Illumina NovaSeq X

platform (Eurofins Genomics, Germany), yielding 30 million 2 × 150 bp paired end reads per sample.

Raw reads were processed using Trimmomatic v0.39 (Bolger et al., 2014) to filter out low-quality reads, adapters, and barcode sequences. Clean reads were aligned to the *Vicia faba* reference genome (Hedin2 v1) (Jayakodi et al., 2023) using the STAR v2.7.11b. Gene expression levels were quantified as raw counts and fragments per kilobase per million reads (FPKM) according to established methods (Trapnell et al., 2012). Principal component analysis (PCA) was performed to assess the correlation between the samples. Genes with low reads were filtered out by retaining only those with a total count ≥ 10 across all samples in each comparison. Differentially expressed genes (DEGs) were identified using the DESeq2 R package with a previously standardized method, applying threshold of $|\log_2(\text{fold change})| \geq 1$ and false discovery rate (FDR) < 0.05 (Benjamini and Hochberg, 1995). To characterize the regulatory components among the DEGs, corresponding peptide sequences were obtained from the annotated *Vicia faba* genome (GCA_948472305.1) and submitted to iTAK v1.6 for TFs, transcriptional regulators (TRs), and kinases.

2.3. Identification of TFs and genes related to flower initiation

To characterize the regulatory components among the DEGs, corresponding peptide sequences were retrieved from the annotated *Vicia faba* genome (GCA_948472305.1) and analyzed using the iTAK v1.6 online tool (http://itak.feilab.net) to classify them as TFs, transcriptional regulators (TRs), and kinases (Zheng et al., 2016). To determine the genetic basis of floral induction differences between the varieties Gubbestad and Honey, we selected a set of flowering-related genes from *Arabidopsis thaliana* models (Bouche et al., 2016; Liu et al., 2024; Wu et al., 2024) and used them as reference sequences to blast against *Vicia faba* reference genome. Subsequently, a reciprocal BLASTP (E-value cutoff 1e-5) was used to mined homologous genes in *Vicia faba* (Altschul et al., 1997), and peptide sequences were further verified by PfamScan (https://www.ebi.ac. uk/Tools/pfa/pfamscan/) to confirm the respective functional domains.

2.4. K-means clustering of DEGs

To analyze the expression patterns of the DEGs, *K*-means clustering was used to group genes with similar expression patterns (Niu et al., 2020). To examine the expression patterns of DEGs associated with flower initiation, *K*-means clustering was performed using the cluster package in R, with Pearson's correlation as the distance metric. The optimal number of clusters (12 for each cultivar) was determined by the gap statistics via the clusGap function in the R package factoextra (Kassambara and Mundt, 2017). Heatmaps were generated using Z-score normalized Log2(FPKM + 1) values and visualized using the pheatmap.

2.5. Weighted gene co-expression network analysis (WGCNA)

Co-expression networks were constructed using the WGCNA package in R to identify co-expression modules and important regulatory genes related to our target trait (Langfelder and Horvath, 2008). Genes with FPKM values greater than one in at least one sample were selected and $\log_2$-transformed prior to downstream analyses. The soft-threshold power was obtained using the pickSoftThreshhold function, ensuring a scale-free topology with $R^2 > 0.9$. To find gene networks associated with floral induction, a gene co-expression network was then constructed to identify gene networks associated with floral induction using the blockwiseModules function, with the following settings: power = 12, minimum module size = 50, TOM type = unsigned, maximum block size = 35000, and merge cut height = 0.25. Regulatory interactions between transcription factors and their downstream genes were predicted using the Plant Transcriptional Regulatory Map (PlantRegMap; http://plantregmap.gao-lab.org) (Tian et al., 2020). Then, the resulting gene regulatory networks were visualized using Cytoscape v3.10.2 (Shannon et al., 2003).

2.6. Gene ontology (GO) and KEGG enrichment analysis

All *Vicia faba* genes were annotated with BLASTP against the Arabidopsis proteome dataset (TAIR11) with an E-value cutoff of 1e−5 (Altschul et al., 1997; Smoot et al., 2011). GO enrichment analysis was performed using the BiNGO plug-in function in Cytoscape version v3.10.4 (Smoot et al., 2011). GO terms with significant enrichment (FDR < 0.05) were identified, and KEGG pathway analysis was subsequently performed using the OmicShare online platform (https://www.omicshare.com/tools). GO results were visualized by generating bubble plots using the ggplot2 package in R (Ginestet, 2011).

2.7. Qualitative real-time time PCR (qRT-PCR) validation

To validate the accuracy of RNA-seq data, qRT-PCR analysis was performed using the same DNase-treated RNA samples and biological replicates as used for RNA-seq. The cDNA was synthesized from 1 μg of total RNA using the Maxima First Strand cDNA Synthesis Kit (Thermo Fisher Scientific, USA) following the manufacturer's instructions. A total of nine flowering-related genes, *AG*, *AGL5/SHP2*, *FT*, *GID1B*, *LFY*, *PI*, *TEM* and two *SOC1*, paralogs, were selected for validation; corresponding primer pair sequences used in qRT-PCR are provided in the table (supplementary Table S7). qRT-PCR reactions were performed using Maxima SYBR Green/ROX qPCR Master Mix (2 X) (Thermo Fisher Scientific, USA). All reactions were conducted in accordance with the Minimum Information for Publication of Quantitative Real-Time PCR Experiments (MIQE) guidelines. Two internal controls, *Actin11* (*VFH.ACT11*) and *elongation factor 1-alpha* (*VFH.ELFA-1*) were used, and relative expression levels were calculated using the $2^{-}\Delta\Delta Ct$ method (Abid et al., 2025; Niu et al., 2020).

3. Results

3.1. RNAseq of two faba bean cultivars with diverse flowering time

Two faba bean cultivars were selected for RNA sequencing based on their contrasting flower initiation phenotypes. The early-flowering cultivar, Gubbestad, initiated flowering 39 days after sowing (DAS; SD = 1.10), whereas the late-flowering cultivar, Honey, flowered at 68 DAS (SD = 1.68) under greenhouse conditions (Fig. 1). It can be noted that days to flowering under field conditions in southern Sweden (Ohm et al., 2024) were very similar for Honey, for greenhouse and field, but slightly longer for Gubbestad in the field. A total of 36 samples (leaf and SA) from the two cultivars at three time points representing distinct biological stages were collected to assess gene expression networks and uncover key regulatory genes associated with flower initiation. To capture the molecular changes associated with the onset of flowering, samples were collected from the vegetative to inflorescence meristem transition stage.

Transcriptome sequencing generated high-quality data, with on average 72.76 million reads per sample and > 75 % uniquely mapped reads, providing sufficient depth for DEGs identification and other downstream analysis for the construction of regulatory network (supplementary Table S1).

3.2. Identification and classification of DEGs

Transcriptome comparisons across three stages: vegetative (21 DAS), early flower initiation (39 DAS), and late flower initiation (68 DAS) in leaf and SA revealed dynamic expression changes associated with flowering initiation in two cultivars. A total of 16,864 unique DEGs were identified across all pairwise comparisons (Fig. 2; supplementary Table S2). In Gubbestad, the transition from the vegetative (G1) to floral

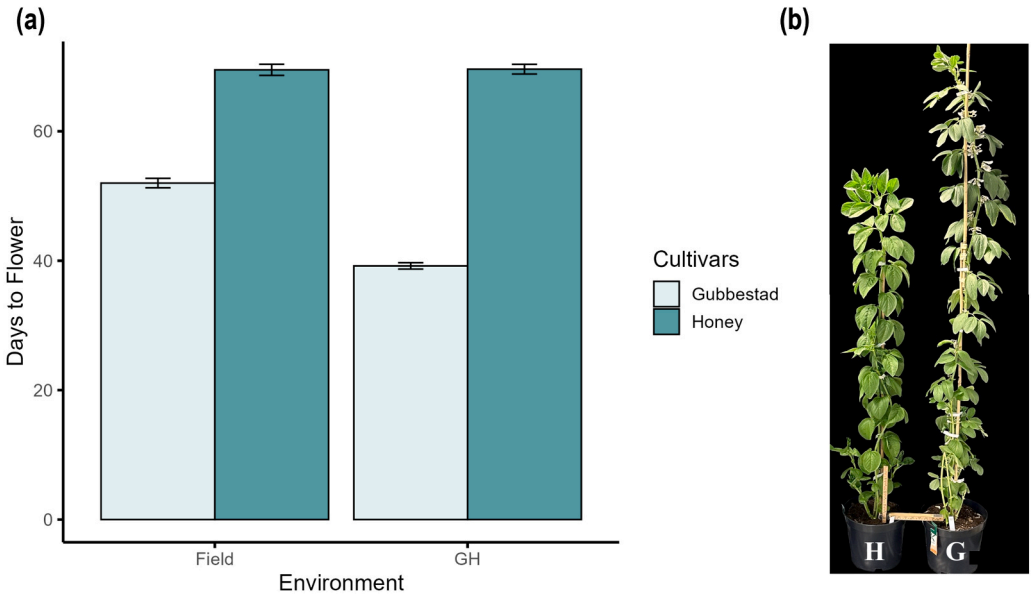

Fig. 1. Days to first flower appearance in field and greenhouse environments. (a) Barplot showing the number of days from sowing to first flower appearance in Honey (H) and Gubbestad (G), grown under field (Ohm et al., 2024) and greenhouse (GH) conditions. (b) Representative plants of the early-flowering cultivar Gubbestad (right) and the late-flowering cultivar Honey (left) photographed when Honey initiated flowering, at which Gubbestad already had open flowers.

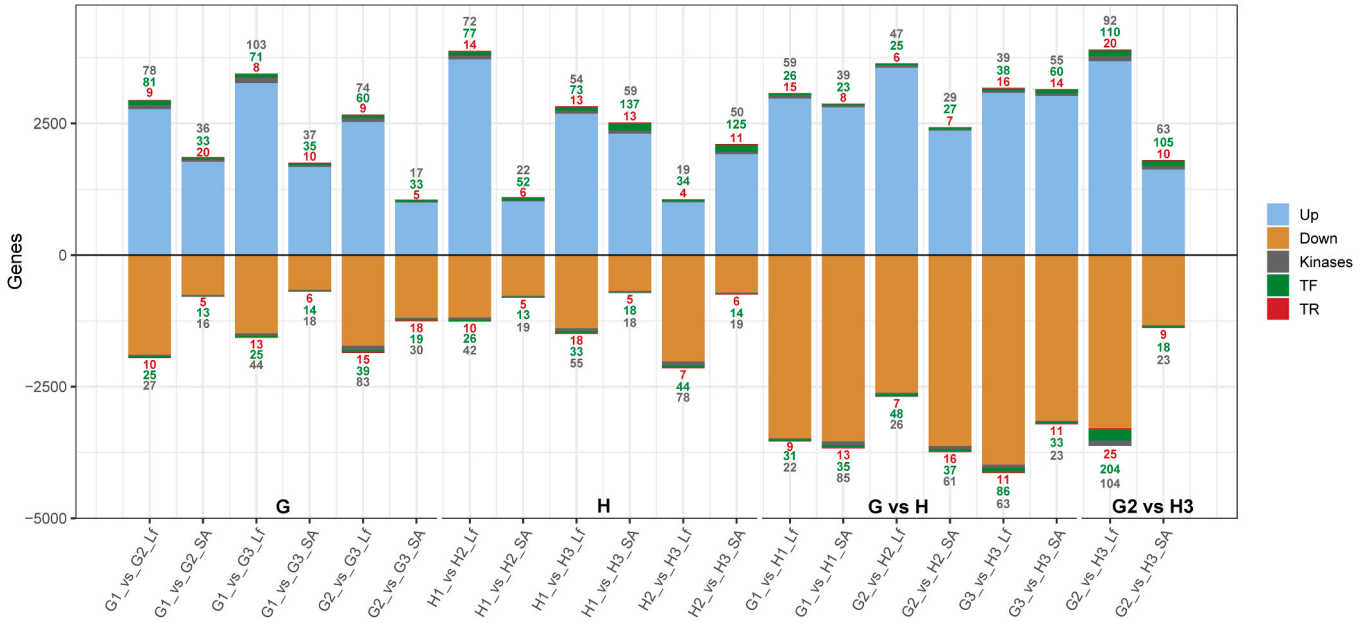

Fig. 2. Differentially expressed genes (DEGs) across stages, tissues and cultivars. DEGs classified as 'Up' or 'Down' were obtained from pairwise comparisons between the cultivars Gubbestad (G) and Honey (H) at three stages (vegetative (1), early flowering (2), and late flowering (3)) in leaf and shoot apex (SA) tissues. The number of Kinases, transcription factors (TFs), and transcriptional regulators (TRs) among the DEGs are shown above/below their respective bars in corresponding colors. Identification of TF, TR, and kinases was carried out via iTAK v1.6 (http://itak.feilab.net) (supplementary Fig. S2; Table S3).

initiation stage (G2) showed strong transcriptional changes, particularly in leaf tissue, where 2776 genes were upregulated and 1896 were downregulated. Although SA had less overall DEGs (1776 up and 759 down), the data set contained a higher proportion of regulatory genes, including more than twice the number of upregulated transcriptional regulators (TRs) in SA (20) than in leaf (9), highlighting their key regulatory role during floral initiation. From G2 to a later flowering stage (G3) DEG numbers declined (leaf: 2527 up / 1723 down; SA: 999 up / 1192 down), suggesting stabilization of transcriptional activity following the transition. The number of TFs in the SA remained relatively stable across both transitions, indicating continued regulatory activity during floral progression.

In Honey, the vegetative stages (H1 vs. H2) showed a substantial number of DEGs in leaf tissue (3717 up / 1187 down), but a more moderate shift in the SA (1021 up / 774 down), indicating that major transcriptional adjustments in the SA had not yet occurred. A pronounced transcriptional shift occurred between H2 and H3, when Honey initiated flowering. At H2 as compared to H3, leaves showed 1005 upregulated and 2022 downregulated genes, while SA showed 1924 upregulated and 713 downregulated genes. Importantly, upregulated TFs and kinases in SA markedly increased between H2 and H3 (125 TFs, 50 kinases) compared with H1 and H2 transition (52 TFs, 22 kinases),

reflecting the regulatory changes accompanying floral initiation.

To explore cultivar-specific expression dynamics, we compared Gubbestad and Honey at their respective developmental stages. At the vegetative stage (G1 vs. H1), the total DEG counts were similar across tissues (leaf: 2975 up / 3482 down; SA: 2805 up / 3540 down). However, the number of TRs and kinases showing higher expression in Gubbestad as compared to Honey was higher in leaf tissue than in SA (TRs, 15 vs. 8, and kinases 59 vs. 39), suggesting earlier engagement of regulatory pathways, particularly in the leaf, potentially contributing to its early-flowering phenotype. At G2 vs. H2, Gubbestad leaves exhibited more upregulated than downregulated genes (3560 up/ 2614 down) compared to Honey. Conversely, at the same time-point comparison between SA showed larger number of downregulated than upregulated genes in Gubbestad (3631 down/ 2366 up), reflecting a developmental shift as the meristem transitioned to flowering, while Honey remained vegetative. These results indicate that leaves show broader transcriptomic changes across stages, while SA plays a more specialized role in flower initiation, particularly in response to developmental cues and genetic mechanisms underlying early and late flowering phenotypes.

In addition, we compared Gubbestad and Honey at their floral initiation stage (G2 and H3, respectively), to capture cultivar differences at comparable developmental stages. This comparison revealed extensive transcriptional differences in both tissues (leaf: 3684 up / 3627 down; SA: 1628 up / 1385 down). Among these DEGs in Gubbestad as compared to in Honey, regulatory genes were strongly represented, with TFs showing particularly large shift in leaf (110 up/ 204 down) and SA (105 up / 18 down) (Fig. 2) indicating that Honey undergoes a major regulatory change at H3 as it initiates flowering.

3.2.1. GO enrichment analysis of DEGs

GO enrichment analysis of DEGs between Gubbestad and Honey, revealed distinct temporal and tissue-specific patterns in gibberellin (GA) and flowering-related processes (supplementary Table S4). Analyses were performed across stages and tissues (leaf and SA), with a particular focus on transcriptional changes during flower initiation.

In leaf tissue, Gubbestad exhibited early enrichment of hormonal and light-responsive terms. At G1, genes related to GA biosynthesis (GO:0009686), GA metabolism (GO:0009685), and response to light intensity (GO:0009642) were enriched. At G2, corresponding to floral initiation in Gubbestad, leaf tissue showed enrichment of genes involved in the cellular response to far-red light (GO:0071490) and specification of floral organ identity (GO:0010093) (supplementary Table S4). In contrast, Honey leaves at H2 were enriched for vegetative-to-reproductive phase transition (GO:0010228), mirroring Gubbestad's earlier response. At H3, Honey leaves showed enrichment in flower development (GO:0009908), negative regulation of short-day photoperiodism (GO:0048577), and GA signaling (GO:0045487), consistent with a late onset of reproductive development.

In SA, transcriptional changes also reflected cultivar-specific timing of flower initiation. In Gubbestad, SA at G1 was enriched for floral meristem growth (GO:0010451), and G2 showed strong enrichment for vegetative-to-reproductive phase transition (GO:0048510) and inflorescence meristem identity (GO:0010077). In Honey, these terms appeared later, with enrichment at G3 in flower development (GO:0009908), GA homeostasis (GO:0010336), response to gibberellin (GO:0009739), and GA-mediated signaling (GO:0010476).

The comparison of the floral initiation stages in the two cultivars (G2 vs. H3) revealed clear differences regarding which biological processes were active. In leaf tissue, genes showing higher expression in Gubbestad as compared to in Honey were enriched for light responsive terms (e.g., GO:0071490, GO:0071490, GO:00102018) consistent with earlier activation of photoperiod-mediated flowering pathways in Gubbestad. In contrast, genes showing higher expression in Honey at H3 were enriched for hormone responsive processes (e.g., GO:0009737, GO:0010371, GO:0090355) and maintenance of inflorescence meristem identity (GO:0010077) reflecting increased hormonal involvement during its later transition to flowering. A similar pattern was observed in SA, with earlier activation of light driven pathways in Gubbestad and increased hormone mediated regulation in Honey as it reaches its flowering transition.

Comparison of adjacent developmental stages within each cultivar further supported these temporal differences. In Gubbestad, DEGs in the transition from G1 to G2 was marked by increased enrichment of GA-related terms (e.g., GO:0010371, GO:0009739, GO:0009685), flowering-related processes (e.g., GO:0009911, GO:0022414, GO:0048506), and photoperiod regulation (e.g., GO:0048573, GO:0048574), particularly in the leaves. In Honey, similar patterns were observed between stages 2 and 3, coinciding with its later floral transition and high enrichment in the SA. In summary, GO enrichment patterns indicate that floral transition occurs earlier in Gubbestad, with photoperiod, hormonal and flowering-related processes activated earlier in leaves, whereas in Honey, these processes appear later and are more prominent in the SA.

3.2.2. K-means clustering reveals expression patterns of DEGs

To categorize DEGs into groups with similar expression profiles, a *K*-means clustering analysis was applied separately to each cultivar and tissue type, resulting in 12 distinct clusters for each case (supplementary Fig. S1a-d). These clusters revealed gene expression patterns that closely correspond to the phenotypic trends of flowering initiation. Notably, we identified gene clusters with expression profiles that aligned with varietal differences in flowering initiation patterns, such as Gubbestad Leaf cluster1 and Honey Leaf cluster7, as well as Gubbestad SA cluster5/6 and Honey SA cluster5 (Fig. 3a, c, f, h and supplementary Fig. S3). These clusters reflect the differential timing of flowering between the early-flowering Gubbestad (with increased expression between stages 1 and 2) and the late-flowering Honey (increased expression between stages 2 and 3).

Gene ontology (GO) analysis of selected clusters further emphasized this distinction, with overlapping terms detected between stage 2 of the early-flowering Gubbestad and the stage 3 of the late-flowering Honey. Both stages mark a shift from vegetative growth to reproductive development, highlighting the shared biological processes during this critical transition. Flowering-related GO terms were observed in important clusters, such as vegetative phase change, flower development, hormone-related terms, aging, photoperiod, and circadian rhythm (Fig. 3b, d, g, i). Heatmap visualization was generated using a subset of genes from the expression clusters known or predicted to be involved in flowering initiation. The results aligned with the clustering patterns, showing an early increase in transcript levels at stage 2 in Gubbestad, in contrast to late expression in Honey, which peaked at stage 3 (Fig. 3e, j). This delayed activation reflects the late onset of flowering-related gene expression in Honey compared to that in Gubbestad. The low or less coordinated expression patterns in Honey leaves likely reflect delayed activation of flowering pathways, whereas the distinct expression pattern in Gubbestad is consistent with its earlier transition to flowering. The limited overlap between flowering-related genes in the leaf heatmap (Fig. 3e) and the SA (Fig. 3j) reflects the distinct biological roles of these tissues during floral induction.

These findings indicate that variations in the timing and intensity of gene expression contribute to the differences in flowering time between the cultivars. Gubbestad transitions to reproductive development by stage 2, whereas Honey remains vegetative until stage 3. This delay in flowering in Honey may be attributed to the late activation of flowering genes.

3.3. WGCNA analysis and co-expression network construction

Transcription factors are key regulators of complex traits in crops, as they govern the expression of downstream genes that contribute to phenotypic variation. To investigate the co-expression networks associated with floral induction, we constructed leaf- and SA-specific gene

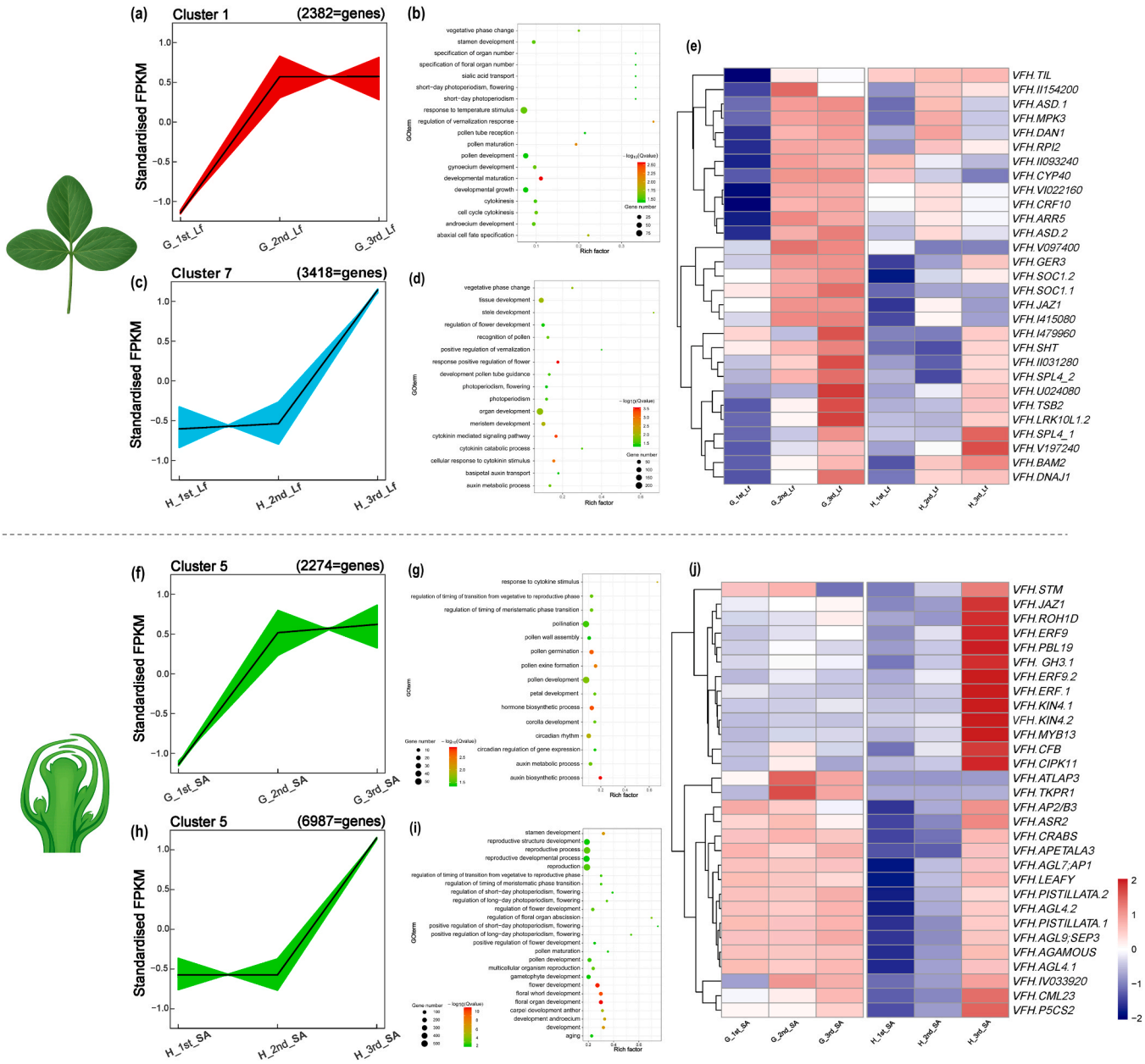

Fig. 3. *K*-means clustering and functional enrichment of DEGs. *K*-means clustering was conducted separately for leaf and SA tissues in Gubbestad and Honey, producing twelve clusters per tissue. Panels (a, c) show selected leaf clusters, and (f, h) show selected SA clusters. The x-axis indicates developmental stage; the y-axis shows standardized FPKM values. Corresponding GO enrichment results are presented in (b, d, g, i). Expression heatmaps of flowering-related genes from two representative clusters in leaf (e) and SA (j) are included. Expression values are based on $\log_2(\text{FPKM} + 1)$.

expression networks using FPKM expression matrices from both cultivars.

The high correlation among biological replicates confirmed the data reliability for network construction (supplementary Figs. S4, S5). Sample clustering showed distinct tissue and stage specific patterns: in leaves stage 2 and stage 3 clustered together in both cultivars, indicate a gradual transition toward flowering, whereas in SA, G2 and H3 formed distinct clusters, consistent with their different flowering times. This pattern reflected the earlier floral transition in Gubbestad and later transition in Honey.

In the WGCNA analysis, the optimal soft-threshold power was determined to be 12 for both leaf and SA tissues, achieving a scale-free topology model fit at $R^2 = 0.9$ (supplementary Figs. S4b, S5b). Using the automatic blockwiseModules function, co-expression modules were identified, resulting in 18 modules for leaf tissue and 16 for SA tissue. Modules were visualized with distinct color schemes to represent the varying levels of gene correlation (supplementary Figs. S4c-d, S5c-d). Functional modules were clearly divisible, with each module exhibiting similar expression patterns concerning stages, cultivars, and flowering time (Fig. 4).

In leaf tissue, across stages, Gubbestad and Honey exhibited different gene expression patterns, with positive and negative correlations with specific color modules, suggesting that these transcriptional profiles are linked to their contrasting flowering behaviors. Highly correlated modules, such as MEblack ($r^2 = 0.95$, $p = 2E{-}09$), MEcyan ($r^2 = -0.80$, $p = 7E{-}05$), and MEblue ($r^2 = 0.99$, $p = 2E{-}17$), were analyzed for GO enrichment. However, significant GO terms related to flowering initiation were only found in MEblack, which revealed GO terms associated with environmental responses, including "response to temperature stimulus" (GO:0009266), "circadian regulation of gene expression"

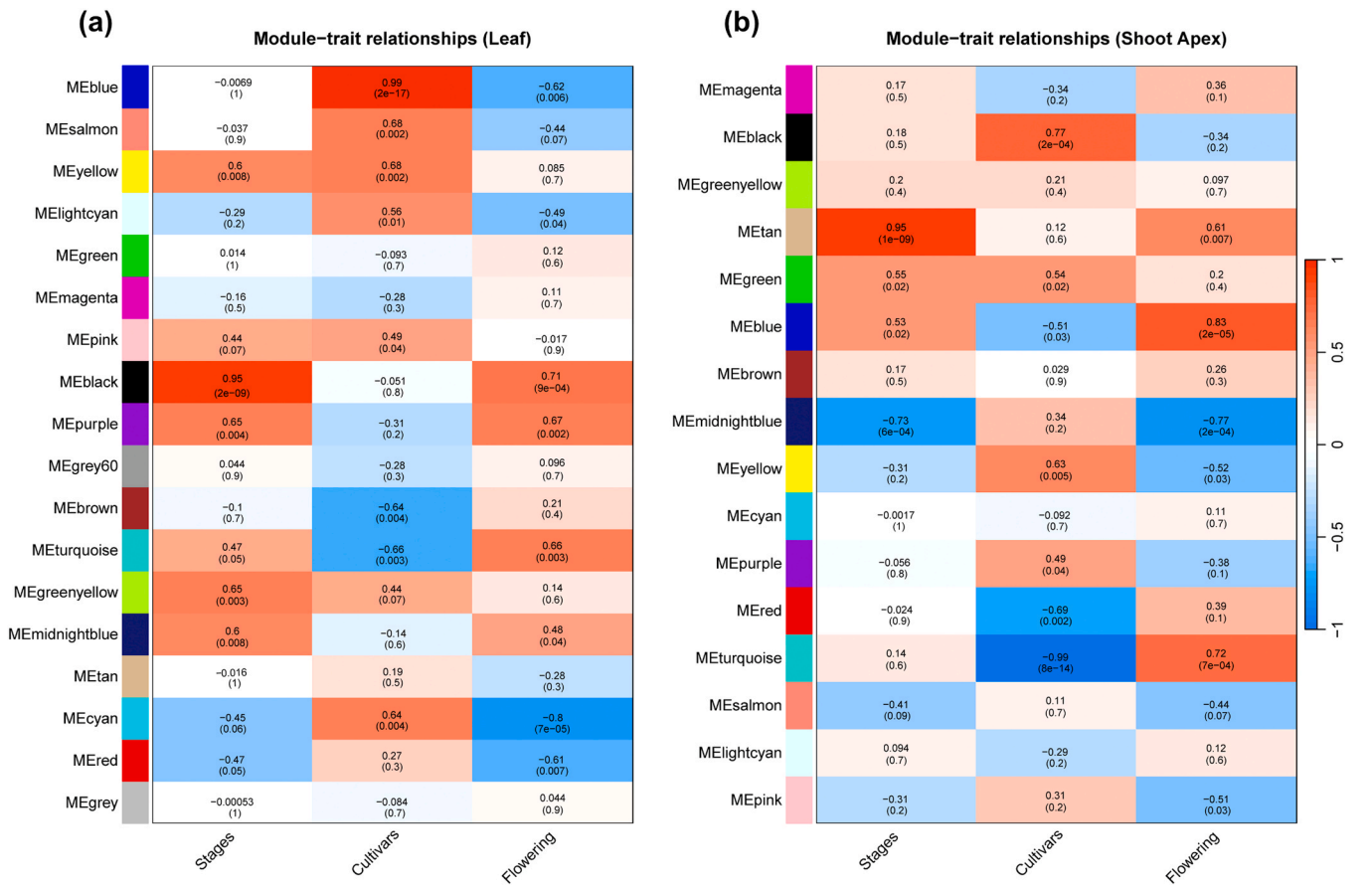

Fig. 4. Module trait relationships in leaf (a) and SA (b). The heatmap illustrates the correlation between colored gene co-expression modules and stages cultivars and flowering time. Each cell displays the correlation coefficient (ranging from –1–1, as indicated by the color scale) along with the corresponding *p*-values.

(GO:0032922), "regulation of circadian rhythm" (GO:0006986), "entrainment of circadian clock" (GO:0009649), and "response to light stimulus" (GO:0009416) (supplementary Fig. S6).

In SA tissue, high correlations were observed in MEblack ($r^2 = 0.95$, $p = 2E{-}09$) for stages, MEturquoise ($r^2 = -0.99$, $p = 8E{-}14$) for cultivars and MEmidnightblue ($r^2 = -0.77$, $p = 2E{-}04$), and MEblue ($r^2 = 0.83$, $p = 2E{-}05$) for flowering time. GO analysis of the highly correlated modules identified MEturquoise and MEblue as particularly relevant to the trait of interest. MEblue was significantly enriched in flowering-related GO terms, including "flower development" (GO:0019219), "floral organ development" (GO:0048437), "reproductive structure development" (GO:0048608), "positive regulation of gibberellic acid-mediated signaling pathway" (GO:0009939), and "maintenance of inflorescence meristem identity" (GO:0010077) (Fig. 5; supplementary Fig. S6).

These findings suggest that the modules contain key regulators of floral initiation, consistent with the phenotypic variations and differential gene expression analyses. MEblack (leaf) was enriched for circadian rhythm, light stimulus, and temperature response, reflecting the environmental regulation of the transition to flowering (Fig. S4). GA-related signaling pathways in MEblue (SA) further support the involvement of hormonal regulation in the initiation flowering. Together, these modules reveal coordinated networks linking environmental cues with GA-mediated developmental signaling.

3.3.1. Co-expression networks and hub genes regulating flower initiation

Co-expression analysis identified two SA derived modules, MEblue ($r^2 = 0.83$, $p = 2E{-}05$) and MEturquoise ($r^2 = -0.99$, $p = 8E{-}14$), as most strongly associated with floral initiation (Fig. 4b). The expression profile of genes within these modules showed high correlation with flower initiation and their respective module eigengene (Fig. 5a, c). A heatmap of these module genes (Fig. 5e) revealed expression dynamics similar to the flowering-related clusters identified by *K*-means clustering (Fig. 3), where flowering genes were upregulated earlier in Gubbestad and later in Honey.

To identify key regulatory genes, hub genes were selected from the MEturquoise and MEblue modules based on gene connectivity (*K*-within) using an absolute Pearson's correlation. Genes within the top 20 % of *K*-within values were designated as hub genes. From the MEturquoise module, 880 genes were selected, with *K*-within values ranging from 782.69 to 1510.33. These genes were classified into 24 TFs, 10 TRs, and 16 kinases (Table S3). The TF *VFH.04SOC1.1* (*VFH.IV033800*) was identified as a key hub gene with a *K*-within value of 1090.23. Its Arabidopsis ortholog, *AT2G45660* (*SOC1*), is a well-characterized regulator of flowering time and a member of the MADS-box TF family.

The gene network associated with *VFH.04SOC1.1* (*SOC1*) consisted of 79 co-expressed genes, including 12 TFs, 4 TRs, and 7 kinases (Fig. 5b; supplementary Table S5). Among these, several genes were associated with vernalization (*VERNALIZATION INDEPENDENCE 5*, *VIP5*), circadian rhythm (*ZINC-FINGER INFLORESCENCE MERISTEM*, *ZIM* ; *CYCLING DOF FACTOR 5*, *CDF5*; *XAP5 CIRCADIAN TIMEKEEPER*, *XCT*), temperature response (*RELATED TO ABI3/VP1 1*, *RAV1*; *TEM1*), and GA signaling (*MYB DOMAIN PROTEIN 65*, *MYB65*). FT and several other flowering initiation and development-related genes were also part of this network. Notably, FT showed high connectivity with the *SOC1* paralog, reflecting coordinated regulatory activity during early floral induction. This co-expression relationship was more pronounced in Gubbestad than Honey, consistent with the earlier activation of flowering pathways in early flowering cultivar.

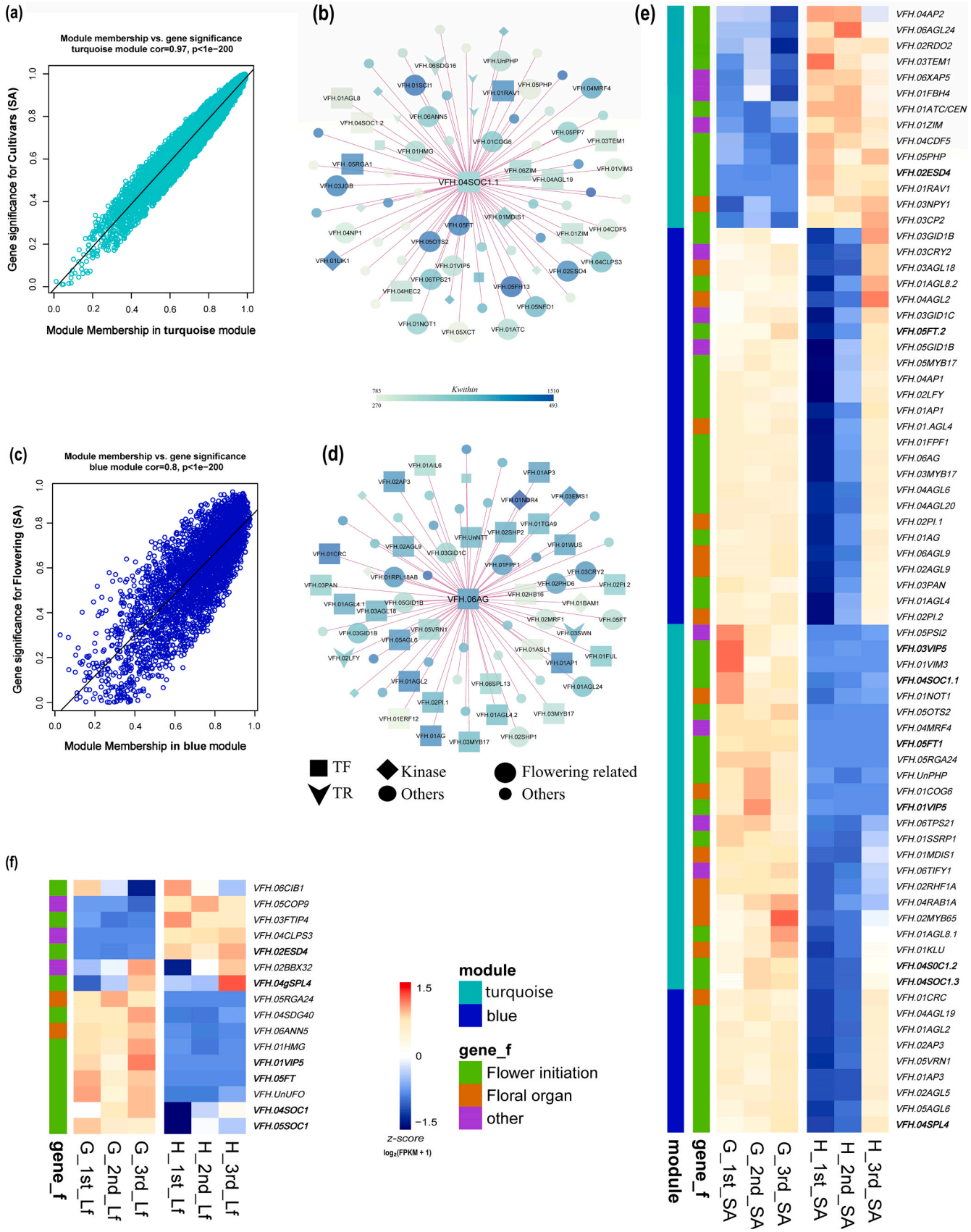

(caption on next page)

Fig. 5. Co-expression network analysis of flowering-related modules identified by WGCNA. The MEturquoise and MEblue modules (derived from SA tissue) were significantly associated with floral initiation. (a) Scatter plot showing the correlation between module membership (gene–module correlation) and gene significance (correlation with cultivar) for the MEturquoise module in the SA. (c) Similar scatter plot for the MEblue module, indicating correlation with flowering-related traits. (b, d) Co-expression networks centered around *VFH.04SOC1* (b) and *VFH.06AG* (d), the hub genes in the MEturquoise and MEblue modules, respectively. Node shapes indicate gene types: squares for transcription factors (TFs), diamonds for kinases, downward arrows for transcriptional regulators (TRs), and circles for other genes. Edge width reflects the strength of co-expression between genes, with wider edges representing higher weight values. (e) Heatmap showing $\log_2$(FPKM + 1) normalized expression (from high (red) to low (blue), see color code) of flowering-related genes from the two modules in SA. Turquoise and blue bars indicate the corresponding gene modules, while gene_f labels denote gene function. (f) Heatmap showing selected flowering-related genes from the leaf tissue.

Similarly, in the MEblue module, 440 genes were selected, with *K*-within ranging from 263.17 to 492.97. Functional classification using iTAK revealed that these genes included 68 TFs, 10 TRs, and 41 kinases (Fig. 5d; supplementary Table S5). The TF *VFH.06AG* (*VFH.VI136800*) was selected as a key hub gene within this module, with a *K*-within value of 439.16. The Arabidopsis ortholog of *VFH.06AG* (*AGAMOUS; AT4G18960*) encodes a MADS-box domain TF, which is known to play a critical role in flower development.

The *VFH.06AG* network consisted of 89 co-expressed genes, comprising 35 TFs, 3 TRs, and 7 kinases (Fig. 5d). This network included floral homeotic genes (*AP1*, *AP3*, *PI*), GA signaling components *GIBBERELLIN INSENSITIVE DWARF1* (*GID1B*, *GID1C*), and members of the MADS-box TF family *SEPALLATA* (*SEP1*, *SEP2*, *SEP3*). The network also included *SPL4*, a miR156-regulated gene, along with several *AGL* genes. Additionally, genes involved in vernalization (*VRN1*), photoperiod regulation (*FT*), and circadian rhythm (*CRYPTOCHROME 2*, *CRY2*) were co-expressed within this network. The presence of multiple flowering-related regulators underscores the significant role of AG in floral organ identity and in reproductive development. Positive regulators of flower initiation (*SOC1*, *FT*, *AG*, etc.) exhibited high expression across all three sampling stages in Gubbestad but were predominantly expressed only at the third stage in Honey (Fig. 5e, f). This pattern indicates late activation of flowering time genes in the late-flowering cultivar.

3.4. Comparative expression analysis of key flowering time genes

The expression of flowering time genes from different regulatory pathways plays a crucial role in floral initiation in response to environmental cues. We observed notable differences in gene expression patterns between the two cultivars, potentially underlying their distinct flowering initiation timings. To compare these genes, expression values were normalized by applying a $\log_2$(FPKM + 1) transformation and Z-score standardization. Based on previously described flower initiation genes in the Flowering Interactive Database (FLOR-ID) and The Arabidopsis Information Resource (TAIR), we selected only those genes that were expressed in at least one developmental stage (Fig. 6; supplementary Table S6). In Fig. 6, each gene is annotated with its corresponding pathway on the left-hand side of the heatmap, indicating hormone related genes such as GA-responsive genes (*GID1B*, *GID1C*, and *RGA24*) as well as photoperiod-related genes (*FT, SOC1*, *CO*, *CRY2*). This visual annotation highlights the coordinated expression of these pathways during floral induction.

Among these selected genes, *VF.05FT.1* was expressed in both tissues (leaf and SA) of the early flowering cultivar Gubbestad but was not detected in any of the tissues in Honey. In contrast *VF.05FT.*2 was expressed only in SA of both cultivars, but expression levels remained higher across all stages in Gubbestad, while in Honey it showed late expression and increased only during the reproductive stage. In the late flowering cultivar Honey, the expression of *TFL1* remained elevated across all SA stages and was markedly higher than in the Gubbestad, consistent with its known role in repressing floral initiation. Similarly, *AP2* genes were highly expressed in the late-flowering cultivar but exhibited reduced expression at the reproductive transition phase. Another circadian rhythm-related gene *Arabidopsis thaliana CENTRORADIALIS* (*ATC*), appeared to promote late flowering in Honey by delaying the floral transition. Most *SOC1* genes followed a similar expression pattern, showing higher expression levels in the early flowering cultivar even at the vegetative stage, whereas in Honey, these genes were only expressed at the flowering stage. The photoperiod-related gene *CRY2* was expressed in both tissues, highlighting its important role in flower initiation. A *TOE1* homolog, known as a floral repressor, was highly expressed in the SA of Honey during the vegetative stage suggesting a role in delaying the floral transition. GA-regulated genes also showed differential expression patterns. The *GIDB* gene, which promotes flower initiation, was highly expressed in Gubbestad at early stages, supporting the early flowering phenotype. Flower development genes, such as *AG* and *RGA24*, appeared to play crucial roles in flower initiation, as they exhibited higher expression at the flowering stage in Gubbestad. Additionally, miR156-regulated *SPL4/5* genes followed a similar pattern, showing high expression at all stages in the early-flowering cultivar. In contrast, in the late-flowering cultivar, these genes displayed a gradual increase in expression towards the flowering stage. Overall, our findings suggest that variations in the expression of important flowering time regulators between cultivars contribute to differences in flowering phenotypes.

3.5. qRT-PCR validation

The relative expression levels of nine key genes were examined using qRT-PCR across three time points in leaf and SA tissues. The resulting expression profiles showed positive correlation with the fold change variations obtained from the RNA-seq results (supplementary Fig. S7). The correlation coefficients between expression levels from qRT-PCR and RNA-seq for the nine DEGs ranged from 0.76 to 0.94 including *VFH.05FT.2* (0.92), *VFH.04SOC1.1* (0.86), and *VFH.03GID1B* (0.88). For genes exhibiting zero FPKM values at specific time points in one or both cultivars, values were adjusted to 0.001 prior to fold-change calculations. Overall, high concordance between relative expression levels from qRT-PCR and RNA-seq measurements was observed for most gene targets, supporting the robustness and reliability of the transcriptomic dataset.

4. Discussion

4.1. Gibberellin dynamics in flower initiation

Flower initiation in *Vicia faba* is a key developmental event that influences seed yield potential, particularly in northern latitudes, where early flowering facilitates maturity within a short growing season. Therefore, understanding the underlying genetic regulation is vital for breeding cultivars with improved climate adaptability and productivity. In this study, we examined the transcriptomic differences underlying flowering time variation in leaf and SA tissues from two contrasting cultivars (Gubbestad and Honey) previously characterized for their flowering time differences (Ohm et al., 2024). WGCNA identified two SA-derived gene modules strongly associated with flower induction (Fig. 5a, c), which were enriched in genes linked to GA signaling and

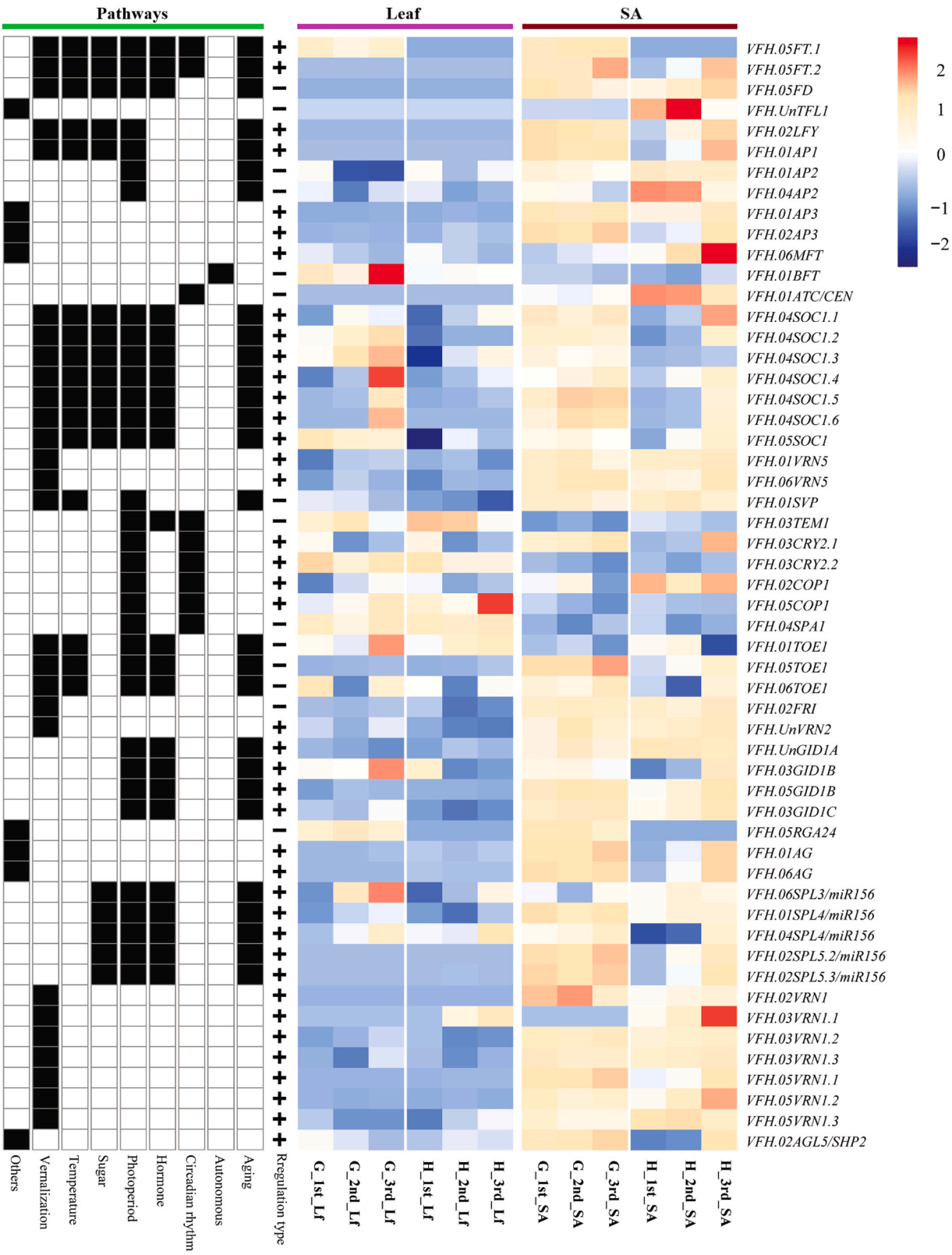

Fig. 6. The expression heatmap of a subset of selected key genes from Arabidopsis involved in regulation of flowering in *Vicia faba* in leaves and SA. The gene expression of both cultivars (G and H) was visualized by Log2(FPKM + 1) transformation, left hand side showing information about pathways and regulation type (+/-) in each gene.

floral development.

K-means clustering further revealed four distinct gene expression clusters, one for each cultivar and tissue type (leaf and SA). While each cluster exhibited unique expression profiles, their overall patterns were consistent with the flowering initiation stages of the two cultivars. Notably, both cultivars shared a similar set of GO-enriched terms at the transition stage (Fig. 3b, d, g, i); however, the flowering related genes were activated later in Honey, aligning with its late floral transition. This temporal difference was also reflected in the DEGs analysis, which showed earlier transcriptional activation in Gubbestad and later in Honey across both tissues (Fig. 2). The limited overlap between flowering-related genes in leaf and SA heatmaps (Fig. 3e, j) was consistent with the distinct biological roles of these tissues, as leaves contribute to the regulation of photoperiod-related flowering signals, whereas SA activates meristem identity and floral developmental programs. A comparative analysis between WGCNA and *K-means* clustering revealed key genes associated with GA-regulated flower initiation, photoperiod response, and floral development. The strong correlation of the expression patterns of these genes and flowering initiation suggests that transcriptional regulation mediated by the GA pathway could be a potential target for fine-tuning of flowering time in *Vicia faba*.

Consistent with previous studies in Arabidopsis, GA-associated genes identified in this study showed expression patterns aligned with pathways where GA is known to promote floral induction by activating *SPL* TF and downstream floral regulators, such as *SOC1* and *LFY* (Bao et al., 2020; Maple et al., 2024; Yu et al., 2012; Zhang et al., 2019). Additionally, GA enhances the expression of *FT* in leaves, a central florigen that integrates multiple flowering signals (Hisamatsu and King, 2008). The enrichment of GA-related GO terms at flower induction, such as Stage 2 in Gubbestad and Stage 3 in Honey in this study, supports the potential role of GA in regulating flowering time. However, a clear distinction was observed between the cultivars, with Gubbestad exhibiting early expression of flower induction genes, ensuring timely flowering, whereas in Honey, the late expression of these genes led to a later floral transition.

These gene expression patterns indicate that GA is associated with tissue-specific regulation of flowering transition in *Vicia faba*: in leaves by inducing *SPL4* and *SOC1*, and in the SA via regulators such as *AGL*, *AP2*, *AP3*, *PISTILLATA* (*PI*), and *LFY* (Fig. 6). The differential gene expression observed between early- and late-flowering cultivars highlights transcriptional regulation as a critical mechanism underlying the variation in flowering time. Taken together, these findings provide transcriptional evidence for GA-associated regulatory changes during floral initiation. However, confirming these mechanisms will require future functional validation of key candidate genes, along with endogenous GA measurement and exogeneous GA application to directly assess hormonal dynamics.

4.2. Hub genes and co-expression networks underlying flower induction

Flower induction is a complex developmental process regulated by the coordinated activity of TFs, hormonal signaling and environmental cues. In this study, WGCNA analysis identified two key co-expression modules in the SA, that showed the highest correlation with flower initiation (Fig. 5a). In these modules, *VFH.04SOC1* and *VFH.06AG* were identified as hub genes, underscoring their potential regulatory role in flower induction (Fig. 5).

SOC1 has been widely recognized as a pivotal integrator of multiple flowering pathways, including those related to GA, vernalization, and photoperiod responses (Kou et al., 2022). In legumes such as *Medicago truncatula*, *SOC1-like* genes, notably *MtSOC1a*, function as key regulators of floral induction, even without the conserved CO-FLC regulatory module that governs flowering in Arabidopsis (Jaudal et al., 2018). In legumes, flowering is regulated by a distinct pathway involving *FT* mediated *SOC1* activation in response to long-day conditions. Moreover, *SOC1* suppresses known floral repressors, such as *TEM1* and *RAV1* (Matias-Hernandez et al., 2014). This study of faba bean suggests that the late flowering trait (Honey) might be associated with low *SOC1* expression and concurrent upregulation of *RAV1* and *TEM1*, indicating that transcriptional repression contributes to late flowering. These insights further emphasize the critical role of *SOC1* as a central molecular regulator of flowering time in *Vicia faba*.

In addition to *SOC1*, the *AG* gene was co-expressed with several key floral induction regulators in the SA, including *AP1*, *AP3*, *SEP*, *SPL4*, and GA receptors *GID1B* and *GID1C*, suggesting their coordinated role in floral initiation. Furthermore, *LFY* and the flowering promoter *FT* were also included in this network. Previous studies have demonstrated that *LFY* and *FT* activate *AP1*, which subsequently promotes the expression of *AG* and *SEP3*, which are crucial for specifying floral meristems and organ identity (Liu et al., 2023; O'Maoiléidigh et al., 2014). The early activation of *FT*, *LFY*, and *AP1* in the SA of the early flowering cultivar (Gubbestad) aligns with previous findings, showing their crucial role in faba bean floral induction (Fig. 7).

Moreover, the early upregulation of several *AGL* TFs in Gubbestad supports their roles in floral transition. Remarkably, *AGL24* has been shown to regulate flowering independently of *SOC1* and *FRUITFUL* (*FUL*), with its expression enhanced under long-day conditions (Huang et al., 2024; Torti and Fornara, 2012). Collectively, these results suggest that floral induction in *Vicia faba* is orchestrated by a complex, interconnected regulatory network of TFs and signaling genes that respond to developmental and environmental cues. This network varies between early- and late-flowering cultivars.

4.3. Regulatory networks governing flower induction in Vicia faba

Flowering regulation has been extensively characterized in Arabidopsis; however, its complexity in legumes, including *Vicia faba*, remains underexplored (Benlloch et al., 2015). Understanding the molecular basis of flowering time variation in legumes is crucial for breeding climate-adapted cultivars that are suited to diverse growing conditions. The expression dynamics of key flowering genes were profiled in early and late flowering *Vicia faba* cultivars to detect conserved and cultivar-specific regulatory patterns (Fig. 6).

Our results highlight the differential expression of *FT*, which is a central floral activator. In Gubbestad, two *FT* homologs were expressed across stages and tissues (leaf and SA), whereas in Honey, only one *FT* homolog was expressed, and only in the reproductive stage of SA. This expression profile aids to the established model in which flower initiation is triggered when *FT* interact with *FD*, whereas *TFL1* antagonizes this activity (Zhu et al., 2020). In Gubbestad, the elevated expression of *FT* likely led to the early up-regulation of *LFY* which is a key gene for floral meristem identity (Fig. 7). This highlights the opposing interaction between *FT* and *TFL1* in the regulation of flowering (Goretti et al., 2020; Hanano and Goto, 2011; Périlleux et al., 2019). Conversely, the late-flowering cultivar exhibited higher expression of *TFL1*, especially during the flowering transition indicating that *TFL1* serves as a major repressor that delays floral induction. In addition, *ATC*, a *TFL1* paralog, showed higher expression in Honey to further support the later flower initiation. Since both *ATC* and *FT* compete for *FD* binding and regulating *AP1* in opposite ways (Huang et al., 2012), this supports a model in which photoperiodic signals modulate functionally divergent *FT* homologs to finely tune floral initiation in faba bean. Furthermore, *AP2*, a key regulator of age-dependent pathways, was highly expressed in Honey, whereas its downstream targets, including *SOC1*, *AP1*, and *SPL*/miR156, were expressed at lower levels. This implies that *AP2* may play an instrumental role in delaying floral transition, through its interaction with *SOC1*, *AG*, and miRNA regulatory pathways (Huang et al., 2012).

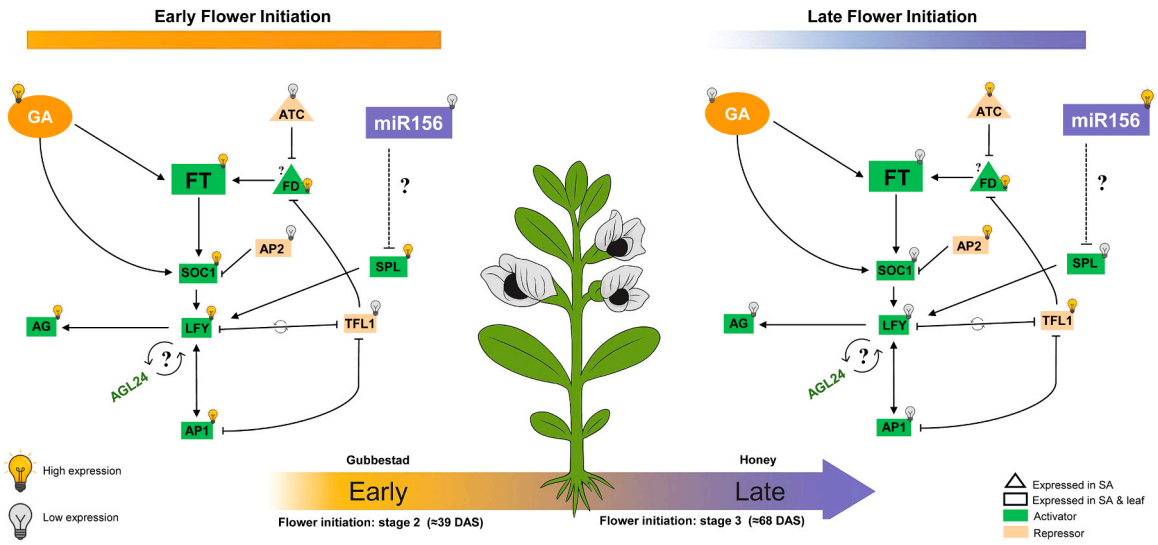

Fig. 7. Proposed model based on transcriptome data explaining early and late flowering in contrasting *Vicia faba* cultivars. This model shows the transcriptional regulation of flower initiation in two *Vicia faba* cultivars. The left panel (Gubbestad) illustrates the early-flowering type, where flower initiation occurs alongside vegetative development, with high expression of floral activator genes (*FT*, *SOC1*, *LFY*, *AP1*, *AG* and *SPL* (*SPL* potentially regulated by miR156)) and low expression of repressor genes (*TFL1*, *ATC* and *AP2*). The right panel (Honey) shows the late-flowering cultivar, with extended vegetative growth and higher expression of repressors and lower expression of activators, as compared to the early-flowering cultivar at the same stage. The model highlights that differences in flowering time arise from shifts in the timing of gene expression, as both cultivars show broadly similar expression once flowering begins.

Overall, these results reveal that flowering in *Vicia faba* is determined by a complex regulatory framework that integrates signals from photoperiod, age, and meristem identity. The contrasting expression of floral activators and repressors between the cultivars highlights the transcriptional basis for their phenotypic divergence. It is essential to functionally validate these regulatory genes to fully understand their specific roles in legume flowering.

5. Conclusion

The regulation of flowering time is a critical determinant of reproductive success and yield stability in *Vicia faba*. This study examined the transcriptional dynamics associated with floral induction in two contrasting cultivars, Gubbestad (early-flowering) and Honey (late-flowering), to identify the molecular mechanisms underlying the differences in flowering time. Through WGCNA and *K*-means clustering, we identified critical regulatory modules enriched in GA-responsive and floral development related genes. These results indicate an association between GA signaling and the expression of transcription factors, such as *SPL*, *SOC1*, *LFY*, and *AGL* during the floral transition.

Gene expression profiling revealed distinct flowering-time regulatory mechanisms between cultivars. The early-flowering Gubbestad exhibited earlier activation of GA-responsive floral genes in both leaves and SA, whereas Honey showed late expression, associated with the upregulation of *TFL1* and *AP2*, both of which act as repressors of floral transition. Notably, *SOC1* was identified as a key hub gene within the WGCNA modules, supporting its conserved role as a floral integrator in legume species. Co-expression analysis also revealed strong interactions between *SOC1*, *AG*, *AP1*, and *FT*, reinforcing their roles in the faba bean floral transition network.

These results provide valuable insights into the genetic and hormonal regulation of flowering time in *Vicia faba* and offer potential targets for breeding programs. Fine-tuning GA-responsive pathways and key transcriptional regulators through plant breeding may enable the development of cultivars that are better adapted to different latitudes and growing season lengths. Future studies should prioritize the functional validation of hub genes and integrate transcriptomic and epigenetic tools to deepen our understanding of flowering regulation in legumes.

CRediT authorship contribution statement

Åsa Grimberg: Writing – review & editing, Validation, Methodology, Funding acquisition, Conceptualization. **Umer Mahmood:** Writing – review & editing, Writing – original draft, Visualization, Methodology, Investigation, Data curation. **Per Hofvander:** Writing – review & editing, Validation, Methodology, Funding acquisition, Conceptualization.

Funding

This study was made possible by funding from Swedish Research Council for Sustainable Development (2021-01767-Formas). Data analyses were performed using UPPMAX computing resources at Uppsala University, part of the Swedish National Infrastructure for Computing (NAISS), under the computing project NAISS 2024/22–328. We also acknowledge the Royal Physiographic Society in Lund, Sweden, for financial support for analytical equipment, and the SLU, LTV faculty for supporting the growth facilities.

Declaration of Competing Interest

The authors have no relevant financial or non-financial interests to disclose.

Appendix A. Supporting information

Supplementary data associated with this article can be found in the online version at doi:10.1016/j.envexpbot.2026.106334.

Data availability

Transcriptome profiling of shoot apex and leaf tissues reveals regulatory networks controlling flowering time in Vicia faba (SRA (NCBI))

References

Abid, G., Sassi, K., Debode, F., Dubois, B., Ouertani, R.N., Abdelkrim, S., Ghouili, E., Gao, Y., Li, Z., Jebara, S.H., Jebara, M., Muhovski, Y., 2025. Comprehensive physiological and transcriptomic insights into drought stress responses in faba bean (*Vicia faba* L.). BMC Plant Biol. 25 (1), 1604. https://doi.org/10.1186/s12870-025-07670-9.

Adamczyk, B.J., Lehti-Shiu, M.D., Fernandez, D.E., 2007. The MADS domain factors *AGL15* and *AGL18* act redundantly as repressors of the floral transition in Arabidopsis. Plant J. 50 (6), 1007–1019. https://doi.org/10.1111/j.1365-313X.2007.03105.x.

Aguilar-Benitez, D., Casimiro-Soriguer, I., Maalouf, F., Torres, A.M., 2021. Linkage mapping and QTL analysis of flowering time in faba bean. Sci. Rep. 11 (1). https://doi.org/10.1038/s41598-021-92680-4.

Altschul, S.F., Madden, T.L., Schaffer, A.A., Zhang, J., Zhang, Z., Miller, W., Lipman, D.J., 1997. Gapped BLAST and PSI-BLAST: a new generation of protein database search programs. Nucleic Acids Res 25 (17), 3389–3402. https://doi.org/10.1093/nar/25.17.3389.

Augustin, M.A., Cole, M.B., 2022. Towards a sustainable food system by design using faba bean protein as an example. Trends Food Sci. Technol. 125, 1–11. https://doi.org/10.1016/j.tifs.2022.04.029.

Bao, S.J., Hua, C.M., Shen, L.S., Yu, H., 2020. New insights into gibberellin signaling in regulating flowering in. J. Integr. Plant Biol. 62 (1), 118–131. https://doi.org/10.1111/jipb.12892.

Benjamini, Y., Hochberg, Y., 1995. Controlling the false discovery rate - a practical and powerful approach to multiple testing (https://doi.org/). J. R. Stat. Soc. Ser. BStat. Methodol. 57 (1), 289–300. https://doi.org/10.1111/j.2517-6161.1995.tb02031.x.

Benlloch, R., Berbel, A., Ali, L., Gohari, G., Millan, T., Madueno, F., 2015. Genetic control of inflorescence architecture in legumes. Front. Plant Sci. 6, 543. https://doi.org/10.3389/fpls.2015.00543.

Blümel, M., Dally, N., Jung, C., 2015. Flowering time regulation in crops - what did we learn from Arabidopsis? Curr. Opin. Biotechnol. 32, 121–129. https://doi.org/10.1016/j.copbio.2014.11.023.

Bolger, A.M., Lohse, M., Usadel, B., 2014. Trimmomatic: a flexible trimmer for Illumina sequence data. Bioinformatics 30 (15), 2114–2120. https://doi.org/10.1093/bioinformatics/btu170.

Bouche, F., Lobet, G., Tocquin, P., Perilleux, C., 2016. FLOR-ID: an interactive database of flowering-time gene networks in Arabidopsis thaliana. Nucleic Acids Res 44 (D1), D1167–1171. https://doi.org/10.1093/nar/gkv1054.

Bunge, A.C., Mazac, R., Clark, M., Wood, A., Gordon, L., 2024. Sustainability benefits of transitioning from current diets to plant-based alternatives or whole-food diets in Sweden. Nat. Commun. 15 (1), 951. https://doi.org/10.1038/s41467-024-45328-6.

Catt, S.C., Braich, S., Kaur, S., Paull, J.G., 2017. QTL detection for flowering time in faba bean and the responses to ambient temperature and photoperiod. Euphytica 213 (6). https://doi.org/10.1007/s10681-017-1910-8.

De Notaris, C., Enggrob, E.E., Olesen, J.E., Sorensen, P., Rasmussen, J., 2023. Faba bean productivity, yield stability and N2-fixation in long-term organic and conventional crop rotations. Field Crops Res. 295. https://doi.org/10.1016/j.fcr.2023.108894.

Dolde, U., Muzzopappa, F., Delesalle, C., Neveu, J., Erdel, F., Vert, G., 2023. LEAFY homeostasis is regulated via ubiquitin-dependent degradation and sequestration in cytoplasmic condensates. Iscience 26 (6). https://doi.org/10.1016/j.isci.2023.106880.

FAOSTAT. 2024. Crops and livestock products. License: CC BY-NC-SA 3.0 IGO. Available online at: ⟨https://www.fao.org/faostat/en/#data/QCL⟩ (Accessed 2025-04-16).

Fernandez, D.E., Wang, C.T., Zheng, Y.M., Adamczyk, B.J., Singhal, R., Hall, P.K., Perry, S.E., 2014. The MADS-Domain Factors AGAMOUS-LIKE15 and AGAMOUS-LIKE18, along with SHORT VEGETATIVE PHASE and AGAMOUS-LIKE24, are necessary to block floral gene expression during the vegetative phase. Plant Physiol. 165 (4), 1591–1603. https://doi.org/10.1104/pp.114.242990.

Ginestet, C., 2011. ggplot2: elegant graphics for data analysis, 245-245. https://doi.org/J. R. Stat. Soc. Ser. aStat. Soc. 174. https://doi.org/10.1111/j.1467-985X.2010.00676_9.x.

Goretti, D., Silvestre, M., Collani, S., Langenecker, T., Méndez, C., Madueño, F., Schmid, M., 2020. TERMINAL FLOWER1 functions as a mobile transcriptional cofactor in the shoot apical meristem. Plant Physiol. 182 (4), 2081–2095. https://doi.org/10.1104/pp.19.00867.

Hall, C., Hillen, C., Robinson, J.G., 2017. Composition, nutritional value, and health benefits of pulses. Cereal Chem. 94 (1), 11–31. https://doi.org/10.1094/Cchem-03-16-0069-Fi.

Hanano, S., Goto, K., 2011. TERMINAL FLOWER1 is involved in the regulation of flowering time and inflorescence development through transcriptional repression. Plant Cell 23 (9), 3172–3184. https://doi.org/10.1105/tpc.111.088641.

Hempel, F.D., Weigel, D., Mandel, M.A., Ditta, G., Zambryski, P.C., Feldman, L.J., Yanofsky, M.F., 1997. Floral determination and expression of floral regulatory genes in Arabidopsis. Development 124 (19), 3845–3853. https://doi.org/10.1242/dev.124.19.3845.

Hisamatsu, T., King, R.W., 2008. The nature of floral signals in Arabidopsis. II. Roles for FLOWERING LOCUS T (FT) and gibberellin. J. Exp. Bot. 59 (14), 3821–3829. https://doi.org/10.1093/jxb/ern232.

Hu, J., Liu, Y.P., Tang, X.H., Rao, H.J., Ren, C.X., Chen, J., Wu, Q.H., Jiang, Y., Geng, F. C., Pei, J., 2020. Transcriptome profiling of the flowering transition in saffron (Crocus sativusL. Sci. Rep. 10 (1). https://doi.org/10.1038/s41598-020-66675-6.

Huang, N.C., Jane, W.N., Chen, J., Yu, T.S., 2012. Arabidopsis thaliana CENTRORADIALIS homologue (ATC) acts systemically to inhibit floral initiation in Arabidopsis. Plant J. 72 (2), 175–184. https://doi.org/10.1111/j.1365-313X.2012.05076.x.

Huang, N.C., Tien, H.C., Yu, T.S., 2024. Arabidopsis leaf-expressed AGAMOUS-LIKE 24 mRNA systemically specifies floral meristem differentiation. N. Phytol. 241 (1), 504–515. https://doi.org/10.1111/nph.19293.

Hyun, Y., Richter, R., Coupland, G., 2017. Competence to flower: age-controlled sensitivity to environmental cues. Plant Physiol. 173 (1), 36–46. https://doi.org/10.1104/pp.16.01523.

Jaudal, M., Zhang, L., Che, C., Hurley, D.G., Thomson, G., Wen, J., Mysore, K.S., Putterill, J., 2016. *MtVRN2* is a Polycomb *VRN 2-like* gene which represses the transition to flowering in the model legume *Medicago truncatula*. Plant J. 86 (2), 145–160.

Jaudal, M., Zhang, L., Che, C., Li, G., Tang, Y., Wen, J., Mysore, K.S., Putterill, J., 2018. A SOC1-like gene MtSOC1a promotes flowering and primary stem elongation in Medicago. J. Exp. Bot. 69 (20), 4867–4880. https://doi.org/10.1093/jxb/ery284.

Jayakodi, M., Golicz, A.A., Kreplak, J., Fechete, L.I., Angra, D., Bednář, P., Bornhofen, E., Zhang, H., Boussageon, R., Kaur, S., Cheung, K., Čížková, J., Gundlach, H., Hallab, A., Imbert, B., Keeble-Gagnère, G., Koblížková, A., Kobrlová, L., Krejči, P., Mouritzen, T.W., Neumann, P., Nadzieja, M., Nielsen, L.K., Novák, P., Orabi, J., Padmarasu, S., Robertson-Shersby-Harvie, T., Robledillo, L.Á., Schiemann, A., Tanskanen, J., Törönen, P., Warsame, A.O., Wittenberg, A.H.J., Himmelbach, A., Aubert, G., Courty, P.-E., Doležel, J., Holm, L.U., Janss, L.L., Khazaei, H., Macas, J., Mascher, M., Smýkal, P., Snowdon, R.J., Stein, N., Stoddard, F.L., Stougaard, J., Tayeh, N., Torres, A.M., Usadel, B., Schubert, I., O'Sullivan, D.M., Schulman, A.H., Andersen, S.U., 2023. The giant diploid faba genome unlocks variation in a global protein crop. Nature 615 (7953), 652–659. https://doi.org/10.1038/s41586-023-05791-5.

Jensen, H.G., Elleby, C., & Domínguez, I.P. 2021. Reducing the European Union's plant protein deficit: options and impacts.

Jordbruksverket. 2024. Jordbruksmarkens användning 2024: Slutlig statistik. Available online at: ⟨https://jordbruksverket.se/om-jordbruksverket/jordbruksverkets-officiella-statistik/jordbruksverkets-statistikrapporter/statistik/2024-10-22-jordbruksmarkens-anvandning-2024.-slutlig-statistik#baljvaxter⟩ (Accessed 2025-07-07).

Karkanis, A., Ntatsi, G., Lepse, L., Fernández, J.A., Vågen, I.M., Rewald, B., Alsina, I., Kronberga, A., Balliu, A., Olle, M., Bodner, G., Dubova, L., Rosa, E., Savvas, D., 2018. Faba bean cultivation - revealing novel managing practices for more sustainable and competitive european cropping systems. Front. Plant Sci. 9. https://doi.org/10.3389/fpls.2018.01115.

Kassambara, A., Mundt, F., 2017. Package 'factoextra'. Extr. Vis. Results Multivar. data Anal. 76 (2), 10–18637.

Kim, J.J., Lee, J.H., Kim, W., Jung, H.S., Huijser, P., Ahn, J.H., 2012. The microRNA156-SQUAMOSA PROMOTER BINDING PROTEIN-LIKE3 module regulates ambient temperature-responsive flowering via FLOWERING LOCUS T in arabidopsis. Plant Physiol. 159 (1), 461–478. https://doi.org/10.1104/pp.111.192369.

Kou, K., Yang, H., Li, H.Y., Fang, C., Chen, L.Y., Yue, L., Nan, H.Y., Kong, L.P., Li, X.M., Wang, F., Wang, J.H., Du, H.P., Yang, Z.Y., Bi, Y.D., Lai, Y.C., Dong, L.D., Cheng, Q., Su, T., Wang, L.S., Kong, F.J., 2022. A functionally divergent SOC1 homolog improves soybean yield and latitudinal adaptation. Curr. Biol. 32 (8), 1728. https://doi.org/10.1016/j.cub.2022.02.046.

Langfelder, P., Horvath, S., 2008. WGCNA: an R package for weighted correlation network analysis. BMC Bioinforma. 9, 559. https://doi.org/10.1186/1471-2105-9-559.

Liu, D., Li, J., Wang, S., Huang, T., Tao, F., Lin, Y., Lin, W., Zhao, X., Huang, Y., Jia, Y., Yang, Z., Luo, C., Zhu, Q., Sung, W.K., Wu, J., Yang, Q.Y., 2024. PlantCFG: a comprehensive database with web tools for analyzing candidate flowering genes in multiple plants. Plant Commun. 5 (2), 100733. https://doi.org/10.1016/j.xplc.2023.100733.

Liu, X., Xing, Q., Liu, X., Muller-Xing, R., 2023. Expression of the populus orthologues of AtYY1, YIN and YANG Activates the floral identity genes AGAMOUS and SEPALLATA3 accelerating floral transition in arabidopsis thaliana. Int. J. Mol. Sci. 24 (8). https://doi.org/10.3390/ijms24087639.

Luo, X., Chen, T., Zeng, X.L., He, D.W., He, Y.H., 2019. Feedback Regulation of FLC by FLOWERING LOCUS T (FT) and FD through a 50 FLC promoter region in arabidopsis. Mol. Plant 12 (3), 285–288. https://doi.org/10.1016/j.molp.2019.01.013.

Lv, X., Zeng, X., Hu, H., Chen, L., Zhang, F., Liu, R., Liu, Y., Zhou, X., Wang, C., Wu, Z., Kim, C., He, Y., Du, J., 2021. Structural insights into the multivalent binding of the Arabidopsis FLOWERING LOCUS T promoter by the CO–NF–Y master transcription factor complex. Plant Cell 33 (4), 1182–1195. https://doi.org/10.1093/plcell/koab016.

Maple, R., Zhu, P., Hepworth, J., Wang, J.W., Dean, C., 2024. Flowering time: from physiology, through genetics to mechanism. Plant Physiol. 195 (1), 190–212. https://doi.org/10.1093/plphys/kiae109.

Mateos, J.L., Madrigal, P., Tsuda, K., Rawat, V., Richter, R., Romera-Branchat, M., Fomara, F., Schneeberger, K., Krajewski, P., Coupland, G., 2015. Combinatorial activities of SHORT VEGETATIVE PHASE and FLOWERING LOCUS C define distinct modes of flowering regulation in. Genome Biol. 16. https://doi.org/10.1186/s13059-015-0597-1.

Matias-Hernandez, L., Aguilar-Jaramillo, A.E., Marin-Gonzalez, E., Suarez-Lopez, P., Pelaz, S., 2014. RAV genes: regulation of floral induction and beyond. Ann. Bot. 114 (7), 1459–1470. https://doi.org/10.1093/aob/mcu069.

Mesfin, S., Gebresamuel, G., Haile, M., Zenebe, A., Desta, G., 2020. Mineral fertilizer demand for optimum biological nitrogen fixation and yield potentials of legumes in northern Ethiopia. Sustainability 12 (16). https://doi.org/10.3390/su12166449.

Moon, J., Suh, S.S., Lee, H., Choi, K.R., Hong, C.B., Paek, N.C., Lee, I., 2003. The *SOC1* MADS-box gene integrates vernalization and gibberellin signals for flowering in

Arabidopsis. Plant J. 35 (5), 613–623. https://doi.org/10.1046/j.1365-313X.2003.01833.x.
Niu, Y., Wu, L.M., Li, Y.H., Huang, H.L., Qian, M.C., Sun, W., Zhu, H., Xu, Y.F., Fan, Y.H., Mahmood, U., Xu, B.B., Zhang, K., Qu, C.M., Li, J.N., Lu, K., 2020. Deciphering the transcriptional regulatory networks that control size, color, and oil content in seeds. Biotechnol. Biofuels 13 (1). https://doi.org/10.1186/s13068-020-01728-6.
Ohm, H., Astrand, J., Ceplitis, A., Bengtsson, D., Hammenhag, C., Chawade, A., Grimberg, A., 2024. Novel SNP markers for flowering and seed quality traits in faba bean (*Vicia faba* L): characterization and GWAS of a diversity panel. Front Plant Sci. 15. https://doi.org/10.3389/fpls.2024.1348014.
Ohm, H., Mahmood, U., Östberg, J., Alverup, J., Grimberg, Å., Hofvander, P., 2025. Comprehensive identification of the PEBP gene family in *Vicia faba* highlighting *VfTFL1a* variation and phenotypic insights into determinate growth. Sci. Rep. 15 (1), 28687. https://doi.org/10.1038/s41598-025-12864-0.
O'Maoiléidigh, D.S., Graciet, E., Wellmer, F., 2014. Genenetworks controlling Arabidopsis thaliana flower development. N. Phytol. 201 (1), 16–30. https://doi.org/10.1111/nph.12444.
Patrick, J.W., Stoddard, F.L., 2010. Physiology of flowering and grain filling in faba bean. Field Crops Res. 115 (3), 234–242. https://doi.org/10.1016/j.fcr.2009.06.005.
Périlleux, C., Bouché, F., Randoux, M., Orman-Ligeza, B., 2019. Turning meristems into fortresses. Trends Plant Sci. 24 (5), 431–442. https://doi.org/10.1016/j.tplants.2019.02.004.
Quiroz, S., Yustis, J.C., Chávez-Hernández, E.C., Martínez, T., Sanchez, M.D., Garay-Arroyo, A., Alvarez-Buylla, E.R., García-Ponce, B., 2021. Beyond the genetic pathways, flowering regulation complexity in. Int. J. Mol. Sci. 22 (11). https://doi.org/10.3390/ijms22115716.
Rehman, S., Bahadur, S., Xia, W., 2023. An overview of floral regulatory genes in annual and perennial plants. Gene 885. https://doi.org/10.1016/j.gene.2023.147699.
Serivichyaswat, P., Ryu, H.S., Kim, W., Kim, S., Chung, K.S., Kim, J.J., Ahn, J.H., 2015. Expression of the floral repressor miRNA156 is Positively Regulated by the AGAMOUS-like Proteins AGL15 and AGL18. Mol. Cells 38 (3), 259–266. https://doi.org/10.14348/molcells.2015.2311.
Shannon, P., Markiel, A., Ozier, O., Baliga, N.S., Wang, J.T., Ramage, D., Amin, N., Schwikowski, B., Ideker, T., 2003. Cytoscape: a software environment for integrated models of biomolecular interaction networks. Genome Res. 13 (11), 2498–2504. https://doi.org/10.1101/gr.1239303.
Shi, Y.Y., Zhang, S.W., Gui, Q.L., Qing, H.W., Li, M., Yi, C.X., Guo, H.Q., Chen, H.B., Xu, J.Z., Ding, F., 2024. The *SOC1* gene plays an important role in regulating litchi flowering time. Genomics 116 (2). https://doi.org/10.1016/j.ygeno.2024.110804.
Smoot, M.E., Ono, K., Ruscheinski, J., Wang, P.L., Ideker, T., 2011. Cytoscape 2.8: new features for data integration and network visualization. Bioinformatics 27 (3), 431–432. https://doi.org/10.1093/bioinformatics/btq675.
Surkova, S.Y., Samsonova, M.G., 2022. Mechanisms of vernalization-induced flowering in legumes. Int. J. Mol. Sci. 23 (17), 9889. https://doi.org/10.3390/ijms23179889.
Tao, Z., Shen, L.S., Liu, C., Liu, L., Yan, Y.Y., Yu, H., 2012. Genome-wide identification of SOC1 and SVP targets during the floral transition in Arabidopsis. Plant J. 70 (4), 549–561. https://doi.org/10.1111/j.1365-313X.2012.04919.x.
Tian, F., Yang, D.C., Meng, Y.Q., Jin, J., Gao, G., 2020. PlantRegMap: charting functional regulatory maps in plants. Nucleic Acids Res. 48 (D1), D1104–D1113. https://doi.org/10.1093/nar/gkz1020.
Torti, S., Fornara, F., 2012. AGL24 acts in concert with SOC1 and FUL during Arabidopsis floral transition. Plant Signal. Behav. 7 (10), 1251–1254. https://doi.org/10.4161/psb.21552.
Trapnell, C., Roberts, A., Goff, L., Pertea, G., Kim, D., Kelley, D.R., Pimentel, H., Salzberg, S.L., Rinn, J.L., Pachter, L., 2012. Differential gene and transcript expression analysis of RNA-seq experiments with TopHat and Cufflinks. Nat. Protoc. 7 (3), 562–578. https://doi.org/10.1038/nprot.2012.016.
Weller, J.L., Ortega, R., 2015. Genetic control of flowering time in legumes. Front. Plant Sci. 6. https://doi.org/10.3389/fpls.2015.00207.
Wellmer, F., Riechmann, J.L., 2010. Gene networks controlling the initiation of flower development. Trends Genet. 26 (12), 519–527. https://doi.org/10.1016/j.tig.2010.09.001.
Wu, X., Liu, Y., Lu, X.F., Tu, L., Gao, Y., Wang, D., Guo, S., Xiao, Y.F., Xiao, P.F., Guo, X.Y., Wang, A.G., Liu, P.F., Zhu, Y.F., Chen, L., Chen, Z.H., 2023. Integration of GWAS, linkage analysis and transcriptome analysis to reveal the genetic basis of flowering time-related traits in maize. Front. Plant Sci. 14. https://doi.org/10.3389/fpls.2023.1145327.
Wu, T., Liu, Z., Yu, T., Zhou, R., Yang, Q., Cao, R., Nie, F., Ma, X., Bai, Y., Song, X., 2024. Flowering genes identification, network analysis, and database construction for 837 plants. Hortic. Res. 11 (4), uhae013. https://doi.org/10.1093/hr/uhae013.
Yoo, S.J., Chung, K.S., Jung, S.H., Yoo, S.Y., Lee, J.S., Ahn, J.H., 2010. Brother of FT AND TFL1 (BFT) has TFL1-like activity and functions redundantly with TFL1 in inflorescence meristem development in Arabidopsis. Plant J. 63 (2), 241–253. https://doi.org/10.1111/j.1365-313X.2010.04234.x.
Yu, S., Galvao, V.C., Zhang, Y.C., Horrer, D., Zhang, T.Q., Hao, Y.H., Feng, Y.Q., Wang, S., Schmid, M., Wang, J.W., 2012. Gibberellin regulates the floral transition through miR156-targeted SQUAMOSA PROMOTER BINDING-LIKE transcription factors. Plant Cell 24 (8), 3320–3332. https://doi.org/10.1105/tpc.112.101014.
Yu, H., Yang, F., Hu, C., Yang, X., Zheng, A., Wang, Y., Tang, Y., He, Y., Lv, M., 2023. Production status and research advancement on root rot disease of faba bean (*Vicia faba* L.) in China. Front Plant Sci. 14, 1165658. https://doi.org/10.3389/fpls.2023.1165658.
Yuan, X.X., Wang, Q., Yan, B., Zhang, J., Xue, C.C., Chen, J.B., Lin, Y., Zhang, X.Y., Shen, W.B., Chen, X., 2021. Single-molecule real-time and illumina-based RNA sequencing data identified vernalization-responsive candidate genes in faba bean (*Vicia faba* L.). Front. Genet. 12. https://doi.org/10.3389/fgene.2021.656137.
Zhang, S., Gottschalk, C., van Nocker, S., 2019. Genetic mechanisms in the repression of flowering by gibberellins in apple (Malus x domestica Borkh.). BMC Genom. 20 (1), 747. https://doi.org/10.1186/s12864-019-6090-6.
Zheng, Y., Jiao, C., Sun, H.H., Rosli, H.G., Pombo, M.A., Zhang, P.F., Banf, M., Dai, X.B., Martin, G.B., Giovannoni, J.J., Zhao, P.X., Rhee, S.Y., Fei, Z.J., 2016. iTAK: a program for genome-wide prediction and classification of plant transcription factors, transcriptional regulators, and protein kinases. Mol. Plant 9 (12), 1667–1670. https://doi.org/10.1016/j.molp.2016.09.014.
Zhu, Y., Klasfeld, S., Jeong, C.W., Jin, R., Goto, K., Yamaguchi, N., Wagner, D., 2020. TERMINAL FLOWER 1-FD complex target genes and competition with FLOWERING LOCUS T. Nat. Commun. 11 (1). https://doi.org/10.1038/s41467-020-18782-1.